Chain Dynamics of Bidisperse Polyethylene Melts: A Monte Carlo Study on a High-Coordination Lattice

Heng Lin,† Wayne L. Mattice,† and Ernst D. von Meerwall*,†,‡

Maurice Morton Institute of Polymer Science and Physics Department, The University of Akron, Akron, Ohio 44325

Received September 8, 2006; Revised Manuscript Received December 5, 2006

ABSTRACT: The dynamics of bidisperse (1K/4.5K) polyethylene (PE) melts in the Rouse-reptation transitional region is studied using a newly designed dynamic Monte Carlo algorithm on a high-coordination (2nnd) lattice. The internal relaxation modes fit the KWW relationship very well. The distinctive dynamic transitions have been identified on the basis of mode analysis. The observed anomalous power law dependence of higher modes agrees very well with other earlier molecular dynamics simulations using united atom models. For the long-chain component in the mixture, the tube dilation concept has been visualized through the short-time diffusion of monomers at different concentration, although the established tube dilation theory seems to be not applicable to this transitional region. The diffusion coefficients have been calculated in real time units over the full concentration range for this mixture of PE. Converting Monte Carlo steps into real time units was based on a previously determined coefficient at the simulation temperature. The results are tested against both the Hess theory generalized by Rathgeber et al. and the von Meerwall/Pearson model. Both models fit our data reasonably well. The two-step relaxation of internal modes predicted by the Hess theory can be vaguely identified in the simulation but cannot be faithfully designated due to the data fluctuation near the zero of the relevant autocorrelation function.

I. Introduction

Computer simulation is an increasingly important tool for predicting the material properties of realistic polymers[1−4] thanks to the more efficient and advanced algorithms[4−8] and faster computers. Many computer models are fast enough to study realistic entangled polymers now.[1,3,4] For example, material properties such as diffusion coefficients and viscosities have been computed and verified by experiments for polyethylene (PE)[2] and polybutadiene,[9] respectively. While most attention has been paid to the monodisperse system in the course of evaluating existing theories, polydisperse systems deserve more considerations in practice because most commercial polymers possess high polydispersity indexes which are often not only the natural result of polymerization reactions but also the critical basis for ease of processing. The importance of polydispersity effects has led to many experimental and theoretical investigations of bidisperse polymer melts,[10−15] which can be regarded as the simplest polydisperse system. However, elucidating the effects of more complex molecular weight distributions can be challenging for existing theories. Computer simulations deal with far less constraints from this prospective. They also retain the ability to access the detailed information on polydisperse polymers, which otherwise may not be accessible to experimental methods. The capability of computing diffusion of individual components in a polydisperse sample is very useful in establishing the relationship between the diffusion distribution and the molecular weight distribution for the petrochemical industry.[16] Furthermore, the weighted sum of the contribution from individual components has been used to estimate the viscosity (η) of a polydisperse sample according the theory.[17,18] As an ongoing effort to better predict the material properties of polydisperse polymers, a recently designed dynamic Monte Carlo algorithm will be used to obtain the diffusion coefficients (D) of individual components in real time units over the full concentration range in this paper.

While the computer simulation is becoming a valuable tool for predicting the material properties of realistic polymers, it has also traditionally been an important device for evaluating theories. For example, computer simulation rendered a strong support to reptation theory and for the first time clearly demonstrated that mean-square displacement $\sim t^{1/4}$ as the result of intermediate slowdown of monomer diffusion due to the tube restriction.[19] While the reptation theory addresses entangled phenomena at the long-chain limit, in the transitional region between the Rouse[20] and reptation[21] dynamics, the strict reptation picture does not hold. On the other hand, computer simulations can provide the detailed information at the transitional region conveniently without invoking the asymptotic limit. There have been alternative theories which cover the Rouse−reptation transition.[22−28] For instance, the Hess theory was designed to provide a full picture of polymer dynamics including the Rouse−reptation transition.[22−24] Comparing to the Rouse theory, the Hess theory has two additional factors. First, the theory no longer adopts the assumption of no excluded volume as the Rouse theory did; instead, there is a range for the effective excluded-volume interaction. Second, the theory sets the entanglement molecular weight M_c. Once the chain length M is longer than the critical entanglement length M_c, the perpendicular motions to the chain contour cease. At this point, the system transits from the Rouse dynamics to reptation dynamics. Rathgeber et al.[26] have generalized the Hess model to the bidisperse system.

Pearson et al. formulated an alternative theory, which is able to treat the entire molecular weight range including the Rouse−reptation transitional region.[25] Their theory considers the overall diffusion as the contribution from both the Rouse dynamics and reptation dynamics, where the reptation dynamics itself consists of the contributions from the strict tube motion and constraint release effect. Von Meerwall et al. later extended the Pearson

* Corresponding author: Ph (330) 927-5904; fax (330) 972-5290; e-mail evm@physics.uakron.edu.
† Maurice Morton Institute of Polymer Science, 44325-3909.
‡ Physics Department, 44325-4001.

10.1021/ma062088s CCC: $37.00
Published on Web 01/11/2007

model by accounting for free volume effects.[27] The von Meerwall/Pearson model has also been conveniently generalized to the bidisperse system. In this work, the microscopic information and macroscopic properties obtained by our model will be used to test these theories.

There have been earlier simulations dealing with polydisperse systems. Baschnagel et al. applied the bond fluctuation model to simulate polymers under both athermal and thermal conditions.[29] Chain lengths were short enough so that in their simulation the entanglement effect can be safely neglected. The radius of gyration of the monodisperse and the bidisperse melts coincided in their study. It was found that the short chains accelerate the long species so that the overall chain length dependence of the diffusion coefficient or the relaxation time is weaker than that of monodisperse melts. Under the thermal condition, the chain conformation deviated from the Gaussian distribution. Experimentally accessible quantities such as ηD were computed over a range of temperatures where η is the zero shear viscosity. Harmandaris et al.[30] also studied the dynamic properties of unentangled PE melts with a polydispersity index of 1.09. However, the objective was not to study how the dynamic properties were affected by polydispersity. Instead, much attention has been paid to the material properties of individual components in the mixture in their work. The D computed using their model is in very good agreement with experimentally measured values. They also found that higher relaxation modes did not conform to the Rouse predictions, which coincided with the results reported by Paul et al. earlier.[6] Barsky studied a slightly entangled bidisperse system using a coarse-grained model based on FENE potentials.[31] It was found that the Hess model fit the data reasonably well in this work. To our knowledge, all previous modeling studies either fall into nonentangled polymer categories or concentrated on generic polymers because simulating realistic polymers inside the entangled regime is computationally demanding. By applying a newly designed two-bead-move algorithm, we were able to investigate long entangled PE chains up to 3−4 M_e with regular desktop computers.[4] The efficiency of dynamic Monte Carlo simulation also enabled big box sizes to be used.

The objective of this paper to study a bidisperse system for PE at 453 K in order to unlock the potential of our model for the precise prediction of dynamic properties of polydisperse samples. Although the validity of our model has been verified by experimental data, our model will be tested again here with other existing computer models and theoretical studies in detail for bidisperse PE melts. In the current simulation, the melts consist of a long-chain component with molecular weight 4.5K and a short-chain component with molecular weight 1K over the full concentration range, and the polydispersity index is as high as 1.68.

The remainder of the paper is organized as follows. In section II we briefly describe the recently designed dynamic Monte Carlo algorithm. In section III the theories representing bidisperse polymer melts are introduced. In section IV the basic static properties and detailed dynamic properties will be discussed. The results will be compared with two theories introduced in section III and with the results of other computer simulations.

II. Simulation Method

Our model has been discussed in detail in the previous paper.[4] The model was based on a high-coordination lattice (2nnd lattice) which arrives by taking out every second lattice site on a diamond lattice. The angles between any pair of the coordination axis of this lattice are 60°. The coordination number of a lattice site is 12.[32] Because of the existence of the underlying diamond lattice, any snapshot obtained by a simulation can be easily reversed back to the atomistic detailed chain.[33] The interaction energy used in this model contains a short-range interaction based on the rotational isomeric state (RIS) model[34] and a long-range interaction energy based on a discretized 6−12 Lennard-Jones (LJ) potential.[35] Both RIS and LJ potentials depend on the type of polymers. The lattice constant corresponds to the real chemical bond length after the type of polymers is decided. In this work, a bead on the lattice represents a two-carbon unit. The distance between the neighboring beads can be calculated using 1.54 Å as a carbon−carbon bond length and 109.5° as a bond angle. The resulting lattice constant is 2.5 Å. Thus, unlike general dynamic Monte Carlo methods, our model is designed to simulate a realistic polymer with chemical details at a finite temperature and at a real experimental density.

In this work, the first-order and second-order energies of RIS potential are $E_\sigma = 2.7$ kJ/mol and $E_\omega = 14.6$ kJ/mol, respectively. In all simulations, not only a 2nnd lattice site cannot be double occupied by beads, but also the underlying diamond lattice does not allow the double occupancy of implicit methylene units, termed as 2nnd "collapse". The parameters for long-range LJ potentials are $\epsilon/k = 185$ K and $\sigma = 4.4$ Å, respectively. Based on these two parameters, the discretized shell energy $U_{L,J}$ can be calculated.[35] Only those of the first two neighboring shells, which represent the repulsive part of the LJ potential, are adopted in our *NVT* simulation as the following: $u_1 = 14.426$ and $u_2 = 0.558$ kJ/mol.

The box size used in the simulation is 30 × 30 × 30 steps (75 Å × 75 Å × 75 Å), in order to exceed twice the root-mean-square radius of gyration, $\langle s^2\rangle_0^{1/2}$, for the long-chain component. The temperature used in all simulations is 453 K. The molecular weight of the long-chain component is 4.5K, while for the short-chain component it is 1K. The size of the periodic box for the simulation is chosen so that the system has the density, ρ, specified by the von Meerwall density model.[36]

$$\rho[T,M_1,M_2,v_1] = [1/\rho_\infty(T) + 2V_E(T)/M^*(v_1)]^{-1} \quad (1)$$

$$1/M^*(v_1) = v_1/M_1 + (1 - v_1)/M_2 \quad (2)$$

$$V_E = 13.93 + 0.06T\ (°C) \quad (3)$$

$$\rho_\infty(T) = 1.142 + 0.00076T\ (°C) \quad (4)$$

The coefficients in the equations have been extracted by fitting a huge amount of *n*-alkane data. v_1 is the volume fraction. M_1 and M_2 are the molecular weights of two components in the mixture. After the calculation, the chain numbers of each component are decided according to the concentration. The beads occupy only about 17−18% of lattice sites in this case for PE.

Single-bead moves and two-bead moves[4] have been used in the simulation in order to reproduce the random and local nature of torsion dynamics. These two local moves allow the moving beads to choose their new configurations from all available sites. The algorithm naturally incorporates the out-of-plane motions and provides many more destinations for moving beads than internal pivot moves. This algorithm represents the stochastic nature of microscopic motions more closely because there is no artificial rule of motion involved. Because of the high

coordination numbers, there are many more distinctive configurations on 2nnd lattice than those on general cubic lattices. For example, in terms of any two consecutive beads on 2nnd lattice, a total of 948 different configurations have been identified and included in a data base for the simulation. In the current simulation, for a single Monte Carlo step (MCS), there is 2/3 probability for a single-bead move and 1/3 probability for a two-bead move. Hence, there is a 1:1 opportunity for every bead to be moved by either single-bead or two-bead moves in every step. The acceptance of single-bead moves and two-bead moves in our simulation is judged by Metropolis rules. Before data could be collected, all simulations have been run long enough to reach equilibration. The signs of reaching equilibration include stabilized average polymer dimensions, large displacements of the center of mass compared to the radius of gyration, and the vanishing of autocorrelation function of the end-to-end vectors. All simulations were conducted on typical desktop computers.

III. Theories for Bidisperse Polymer Melts in the Transitional Regime

The Hess theory is one of the several theories which may be applicable to our system. It has been extended and thoroughly checked by Rathgeber and co-workers recently.[26] Favorable agreements have been reached according to their studies. The Hess theory itself is a generalized Rouse model, which describes the microscopic dynamics of polymer melts. Unlike the Rouse model, the Hess model introduced excluded volume effects, which appear as an additional memory function of entanglement friction resulting from the surrounding chains other than the test chain in the generalized Langevin equation. Through the excluded volume effects in the Hess model, both motions of the test chain and the surrounding chains contribute to the relaxation of the entanglement friction function, which implicitly incorporates the constraint release effects. Here only the important conclusion of the generalized Hess theory is covered in the following paragraph.

The overall center-of-mass diffusion in the Hess model can be successfully decoupled into the contribution of curvilinear diffusion $D^{\parallel}$ along the chain contour and $D^{\perp}$, which is perpendicular to the chain contour.

$$D_i = \left(\frac{1}{D_i^{\mathrm{R}}} + \frac{\varphi}{3kTV} \sum_{i' \neq i} \frac{N_{i'} N_i}{D_{i'}^{\perp} + D_i^{\perp} + D_{i'}^{\parallel} + D_i^{\parallel}} \right)^{-1} \tag{5}$$

φ is the mean excluded-volume energy between two arbitrary segments. D^{R} is the Rouse diffusion coefficient. For monodisperse polymer melts, the analytical solution of the equation exists:

$$\begin{aligned} D^{\perp} &= \frac{2}{3}\left(\frac{1}{D_{\mathrm{R}}} + \frac{N\varphi}{6kTVD^{\perp}} \right)^{-1} \\ &= \frac{2D_{\mathrm{R}}}{3}\left(1 - \frac{N}{N_{\mathrm{c}}} \right) \quad \text{for } N \leq N_{\mathrm{c}} \\ &= 0 \quad \text{for } N \geq N_{\mathrm{c}} \end{aligned} \tag{6}$$

Above the critical degree of polymerization N_{c}, the perpendicular motion freezes and only curvilinear motion exists. Rathgeber et al. generalized the formula for the transitional region for a bidisperse system, where the numbers of segments per molecule are $N_t > N_m$.[26]

$$\begin{aligned} D_t &= D_t^{\mathrm{R}}\left(1 + 2\Phi_t \frac{N_t}{N_{\mathrm{c}}} + \frac{4(1-\Phi_t)N_t N_m}{N_{\mathrm{c}}(N_m + 3N_t) - 2N_t N_m(1+\Phi_t)} \right)^{-1} \\ &\qquad \text{for } \Phi_t \leq \frac{N_{\mathrm{c}}}{N_m} - 1 \\ &= D_t^{\mathrm{R}}\left(1 + 2\Phi_t \frac{N_t}{N_{\mathrm{c}}} + \frac{4(1-\Phi_t)N_t N_m}{N_{\mathrm{c}}(N_t + N_m)} \right)^{-1} \quad \text{for } \Phi_t \geq \frac{N_{\mathrm{c}}}{N_m} - 1 \end{aligned} \tag{7}$$

In this formula, Φ_t is the concentration of the entangled long chain. There is no adjustable parameter once D^{R} is decided and the critical entanglement molecular weight is fixed.

There is another important conclusion in the generalized Hess theory that predicted the two-step function of time correlation function of normal modes for the higher modes as seen in the literature.[26] This two-step relaxation will be checked in following discussions. Note the two-step transition happens at the very low value of the autocorrelation function which is close to zero. We will find later that this very fact induces a significant difficulty for comparisons.

Pearson et al. formulated an alternative theory,[25] which is able to treat the entire molecular weight range and nicely covers the transition region from the Rouse dynamics to the reptation dynamics. Pearson's theory considers the overall diffusion from the contributions from both the Rouse dynamics and entangled dynamics: $D = [1/D_{\mathrm{Rouse}} + 1/D_{\mathrm{ent}}]^{-1}$, where $D_{\mathrm{Rouse}} = d_0/M$ and $D_{\mathrm{ent}} = D_{\mathrm{rep}} + D_{\mathrm{CR}}$. D_{rep} and D_{CR} are contributions from strict reptation and constraint release, respectively. $D_{\mathrm{CR}} = \alpha D_{\mathrm{rep}}(M_{\mathrm{c}}/M)^2$ where $\alpha \approx 15$ and $D_{\mathrm{rep}} = d_1/M^2$. It can be shown that

$$D(\text{any } M) \leftarrow D(\text{unent})\left\{ 1 + \frac{M}{R[1 + \alpha(M_{\mathrm{c}}/M^2)]} \right\}^{-1} \tag{8}$$

where $R = d_1/d_0$. D(unent) is the diffusion coefficient in absence of entanglement effects. Neither the Pearson theory nor the Hess theory explicitly considered the chain ends effects or the contour length fluctuation (CLF) effect. For marginally entangled polymers near the transitional region, CLF may not be omitted. For the correction of chain end effects, von Meerwall et al. formulated an approach by applying free volume theory.[26] For a bimodal polymer melt, the diffusion coefficient D_i ($i = 1, 2$) can be calculated from eq 9 and inserted into D(unent).

$$D_i(T, M_1, M_2, v_1) = A \exp(-E_a/RT) M_i^{-1} \exp[-B_d/f(T, M_1, M_2, v_1)] \tag{9}$$

Coefficients A, B_d, and activation energy E_a inside the equation have been extracted by fitting a large amount of data for *n*-alkanes. f is the fraction of free volume indicated by eq 10:

$$f(T, M_1, M_2, v_1) = f_\infty(T) + 2V_E(T)\rho[T, M^*(v_1)]/M^*(v_1) \tag{10}$$

where M^* and ρ have been given in eqs 1−4. Note that in the treatments above no tube dilation has been incorporated. Both d_1 and M_{c} are concentration-dependent values. Thus, the following relationship incorporating tube dilation is still needed.

$$M_{\mathrm{c}}(v_1) = M_{\mathrm{c}}^0/(1 - v_1) \tag{11}$$

$$R(v_1) = R^0 M_{\mathrm{c}}(v_1)/M_{\mathrm{c}}^0 \tag{12}$$

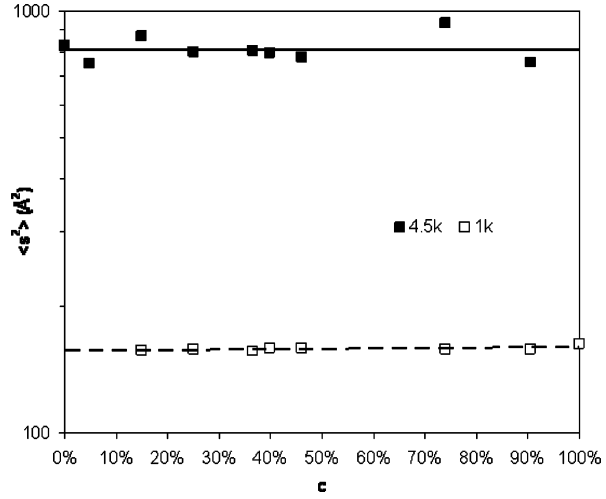

Figure 1. Mean-square radius of gyration $\langle s^2 \rangle$ of long-chain and short-chain components in the mixture against the weight concentration of short chains.

The theory above must also satisfy the limiting condition when $\upsilon_1 = 1$, which is the infinitely dilute condition. The multiplicative correction to D_2 described by von Meerwall et al.[27] has been applied. That correction, eq 13, has little effect at $\upsilon_1 < 0.9$ but produces the desired result at $\upsilon_1 \approx 1$.[27]

$$D_2(\text{dilute}) = D_2(\text{concentrated})\{1 + \upsilon_1^4[(M_2/M_1)^{0.3} - 1]\} \tag{13}$$

Now the diffusion coefficients can be calculated for PE over the full concentration range of both long- and short-chain components.

IV. Results and Discussion

In this paper, our attention will be paid mainly to investigating entanglement phenomena in the bidisperse melts because the Rouse regime has been more or less covered by several other papers mentioned in section II. Based on the fact that short chains are similar to the Θ solvent of entangled long chains, the rest of the discussion will be overwhelmingly on the long component unless another specific indication has been made. Another reminder is that the concentration here refers to the weight concentration c of the short component in order to follow the tradition of earlier publications by our group.[27] Some prior literature cited earlier uses the long component concentration, which corresponds to Φ written in this work.

A. Static Properties. The static properties of both the long and short components have been checked. A plot of their dimensions vs c is given in Figure 1. As expected, no systematic dimension change has been found, and the short component may be regarded as the Θ solvent of the long component. When there is a vast difference between the lengths of two components, a change of chain dimensions may occur. In the current system, no significant change of chain dimensions has been observed.

B. Mode Analysis. According to the theory, the trajectory of a Gaussian chain can be decomposed into the Rouse modes:[18]

$$x_p = \frac{1}{n}\sum_{n=1}^{N} r_n(t) \cos\left(\frac{pn\pi}{N}\right) \tag{14}$$

N is the number of repeating units, and $r_n(t)$ is the position vector at the time t. p is 1, 2, ..., etc. Each of these modes x_p is independent, which is able to describe the dynamics of the chain

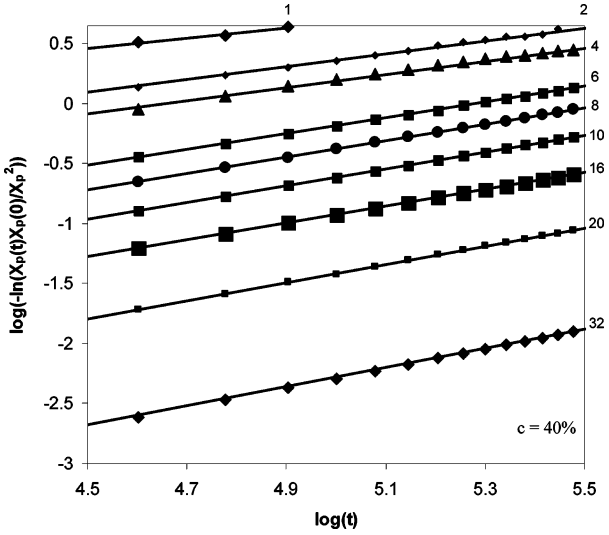

Figure 2. Normal modes fitting of long-chain components according to the KWW equation when $c = 0.4$.

involving N/p segments. The bond length and persistence length are the same in a freely jointed chain. However, the short-range intramolecular correlations in polyethylene, which are incorporated in our simulation, cause our chain to have a persistence length that is about 2.5 times larger than the step length on the high-coordination lattice. This local stiffness implies a possible correlation in the very high p Rouse modes in our simulation.

From the molecular simulation, this quantity can be calculated directly from the time-dependent coordinates of all beads. According to the Rouse theory, the normalized time correlation function of normal modes is an exponential decay.

$$\langle x_p(t)\, x_p(0)\rangle / \langle x_p^2 \rangle = \exp(-(t/\tau)) \tag{15}$$

The realistic chains, either entangled or unentangled, do not necessarily follow this relationship exactly. A common approach[37] uses a KWW equation in the form

$$\langle x_p(t)\, x_p(0)\rangle / \langle x_p^2 \rangle = \exp(-(t/\tau)^\beta) \tag{16}$$

The normalized time correlation functions of the normal modes are shown in Figure 2 for the longer component in the mixture. p is 1, 2, 4, 6, 8, 10, 16, 20, and 32. After a simple mathematical transformation as shown in Figure 2, the autocorrelation function can be conveniently fitted with a linear relationship. From the fitting, two important parameters τ and β in the KWW equation can be obtained. The effective relaxation time τ_{eff} can be calculated using eq 17

$$\tau_{\text{eff}} = \int_0^\infty \exp[-(t/\tau)^\beta]\, \mathrm{d}t = \frac{\tau}{\beta}\Gamma(1/\beta) \tag{17}$$

where $\Gamma(x)$ is the gamma function

$$\Gamma(z) = \int_0^\infty t^{z-1} \mathrm{e}^{-t}\, \mathrm{d}t \tag{18}$$

For each concentration in this work, at least nine normalized correlation functions of modes have been calculated, and the KWW fitting has been done in the same way as shown in Figure 2. The data of monodisperse PE melts at several different chain lengths have also been included and analyzed in the same way for a better comparison. The data fitting results of monodisperse melts are shown in Figure 3. The data fitting for bidisperse

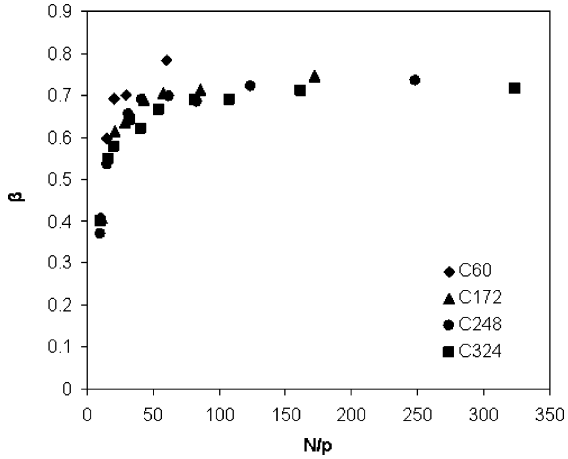

Figure 3. β in KWW equation for monodisperse systems at different molecular weights vs N/p.

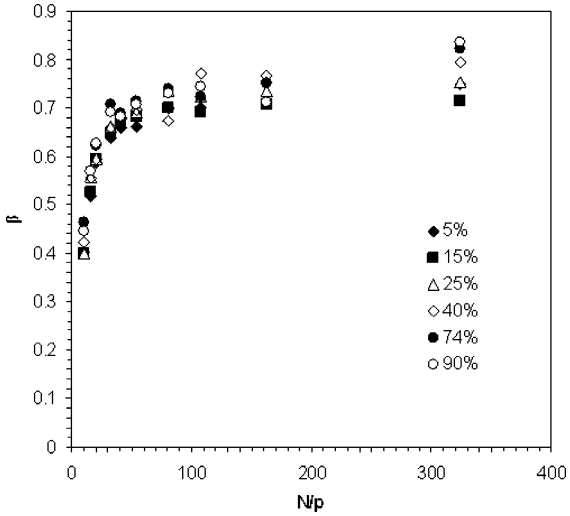

Figure 4. β extracted from the normal mode fitting of long-chain components in the mixtures according to the KWW equation, at the indicated value of c.

mixtures is shown in Figure 4. Note N here is carbon number instead of 2nnd bead number. (One 2nnd bead has two carbon atoms.)

In Figure 3, when β from those chains in monodisperse melts is plotted against N/p, a master curve appears. β increases rapidly against chain segment length N/p initially and starts leveling off at 0.7, except for unentangled C60. In the case of C60, β continues rising to 0.8. According to Shaffer and the references therein,[37] a low β value generally signifies the strong constraints of the dynamics, however according to the reptation theory; chains shall move according to the Rouse dynamics below the length scale of entanglements. Only around the entanglement length, the additional tube constraint sets in and stays until the probe chain fully relaxes itself. This seemingly contradicts our observation here. Of course, the reptation theory is a generic theory which did not take local stiffness effects into account. Therefore, it is natural to consider the low β at the short distance scale as a consequence of local intrachain interactions, i.e., the stiffness. No similar behavior has been found in Shaffer's work, probably because his model did not include the realistic intrachain interactions either. On the other hand, a similar behavior has been found by Padding et al.,[1] whose model did include certain intrachain interactions. Once this intrachain interaction is screened out, a plateau arrives. Thus, the transition point of β may symbolize the blob size in a dynamic sense.

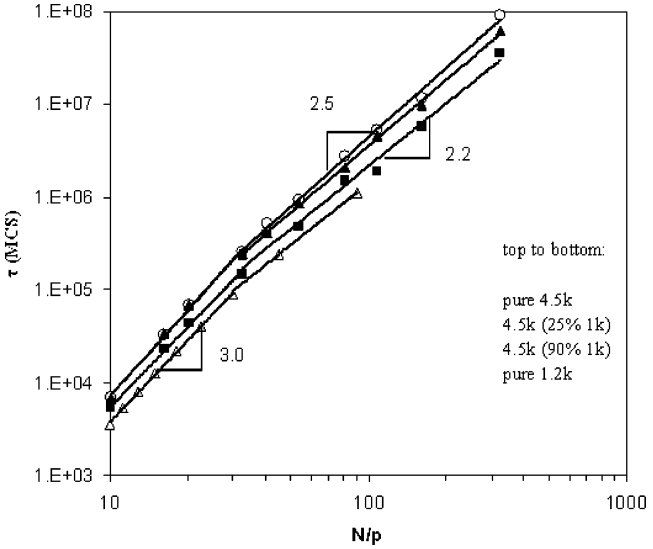

Figure 5. Effective relaxation times from normal modes fitting of long-chain components in the mixture and pure components according to the KWW equation.

However, there was a different interpretation of this transition in the literature. Padding et al. identified the transition as the critical entanglement length M_c.[1,37] This interpretation may gain support from our results as well because β of unentangled C60 did not reach a plateau but longer entangled chains did. More interestingly, Padding et al. also identified a minimum for β before the transition point, which they considered as a new length scale, termed as slowdown length N_s. This new length scale is not observed in our results.

Similar results for the long component for six bidisperse mixtures are plotted in Figure 4. One contrast to the monodisperse system is that the plateau was only reached by mixtures rich in the long component (short chain component below 25%). Like C60, β of dilute solutions increases with the length scale, which Shaffer interpreted as a relaxation toward less constrained dynamics. Unlike the initial rise of β at small N/p, suggesting a master curve due to intrachain interactions, the following rise of β of dilute mixture at larger N/p spread out, depending on the concentration. This rise in the second stage should correspond to intermolecular interactions. Of course, a much more interesting query is "how does the β plateau relate to the entanglement phenomena?" In fact, de Gennes has pointed out[38] that β in the KWW equation is not just a fitting parameter irrelevant to the underlying physics of polymer relaxation processes. Instead, β may closely connect to the entanglement phenomena. The exact nature of this relationship is still an open question.

Now attention is turned to the effective relaxation time τ_{eff} extracted from the KWW equation. In Figure 5 τ_{eff} is plotted against N/p. The relaxation time is expected to scale as $(N/p)^2$ according to the Rouse model. However, at the short length scale this is clearly not the case. Instead, it can be seen that $\tau \sim (N/p)^3$ in the initial stage, which may correspond to the earlier findings of unexpected small β values at this region. The Rouse dynamics is not an accurate description at the short distance scale, and the true dynamics is more complicated than the Rouse prediction because of the factors such as the stiffness effect or intermolecular interactions at the short distance scale. For example, a brief discussion has been given earlier[4] to the subdiffusive behavior of the center of mass at the short distance or time scale. Instead of the Rouse predicted slope, 1, a slope 0.83 has been identified for either unentangled or entangled

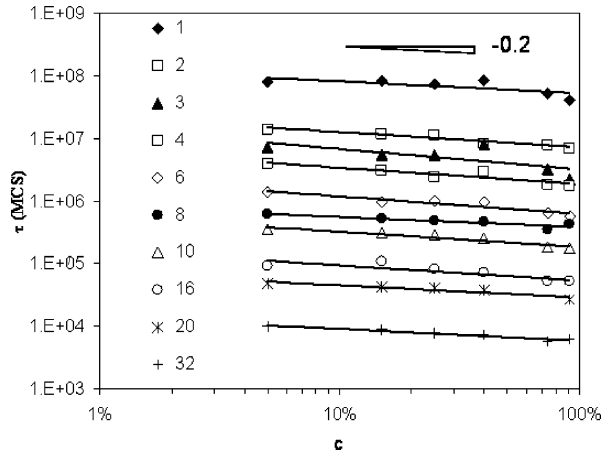

Figure 6. Effective relaxation times from normal modes fitting of long-chain components in the mixture plotted against the concentration of the short chain.

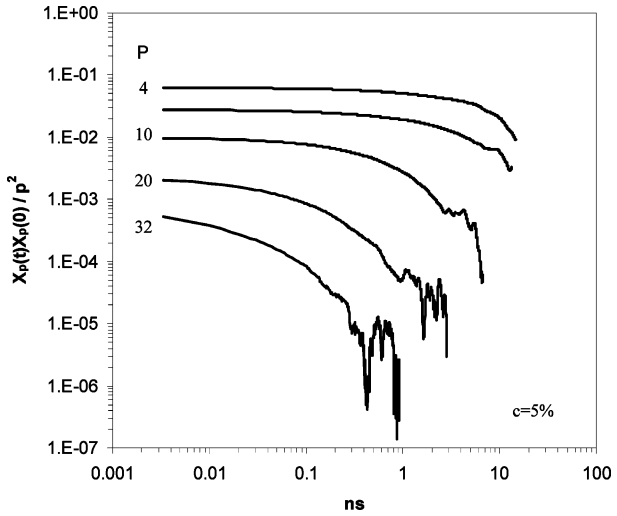

Figure 7. Normal-mode analysis of long-chain components in the mixture plotted against the time in searching for the two-step relaxation predicted by the Hess theory.

chains. Furthermore, there were repeated observations from united atom MD simulation of unentangled PE[6,30] showing that, at the short time and distance scale, normal mode $\langle x_p^2(0)\rangle \sim 1/p^3$ instead of predicted $1/p^2$. The same observation has not been found in the coarse-grained bead−spring model, which may be understandable because it is not designed to represent true conformation and dynamic environment below its coarse-grained level. Note the MD simulations mentioned above took a standard Rouse approach to analyze their data, while a different approach (KWW) is used here for a better coverage of our data. These two approaches may not conflict with each other because, as we have shown,[4] for relatively short unentangled PE chains both the KWW equation and Rouse model could fit the data very well. The fact that our model reaches the same conclusion here as previous MD simulations did proves that our dynamic Monte Carlo simulation based on an RIS model of PE on 2nnd lattice is robust and can be comparable to atomistic MD simulations.

In Figure 5, after N/p increases to the point around 30, a Rouse-like scaling recovers for the unentangled chain with $M = 1.2$K in the monodisperse melt. However, for the monodisperse melt with $M = 4.5$K, an intermediate slope 2.5 shows up. The interpretation should be careful here because if the intermediate slope signifies the onset of entanglements, then the transition to the entangled dynamics is too early for $N/p \sim 30$ if compared with $N_c = 110$ obtained in our earlier work. The ideal picture of this figure should include two transitions for entangled PE. The first transition is from slope 3 to slope 2, and the second transition is from slope 2 back to 3 or some higher value such as 3.4. This is to say, between the short distance (or time) scale dynamics and the entanglement dynamics, one should expect an intermediate region dominated by Rouse dynamics, and only after this region, an upward trend with slope bigger than 2 is expected. In Figure 5, the first transition from the local dynamics to the Rouse dynamics is seen. The data presented here are still too few and too scattered to tell whether there is a secondary transition toward the entanglement dynamics, especially since the longest chain (4.5K) in this work cannot be considered as a fully entangled melt. In between the two pure samples, the long component in the mixture shows intermediate slopes which should be reasonable results.

The τ_{eff} of the long component in the mixture has also been plotted against the concentration in Figure 6. The nominal concentration dependence is $\tau_{\text{eff}} \sim c^{-0.2} \sim (1 - \Phi)^{-0.2}$, where c is the short-chain concentration and Φ is the long-chain concentration. If τ_{eff} is directly plotted against Φ as seen in the literature which generally discuss the very long entangled chain in its Θ solution, then the concentration dependence is way below the prediction of theory[14] and experimental results: $D \sim M^2\varphi^{-1.75}$. The major difference here is that our chain length corresponds to the initial part of the broad transition from the unentangled to entangled dynamics, which is seldom considered in the original tube model which emphasizes long-chain limit all the time. Another difference is that the chain lengths of two components here are pretty close to each other. These are the reasons why we have only discussed the theories which are able to nicely cover the unentangled−entangled crossover in the beginning of this paper. The traditional tube dilation theory for Θ solution of the entangled long chains which predicts $D \sim M^2\varphi^{-1.75}$ would not be applicable for our system. Of course, our simulation does not invalidate the theory either.

As a result, the Hess theory discussed earlier is used here to compare our results. The predicted step function of relaxation of normal modes is checked first. In order for the convenient comparison with the theory and future experimental results, the MCS was converted into real time *ns* using the coefficient (330 MCS = 1 ps) obtained previously.[4] In Figure 7, it seems there is a step transition for the relaxation of higher modes; however, data scatter a lot for the second stage. As mentioned earlier, the Hess theory predicted that the step transition happens near a value of zero for the autocorrelation function, which poses a significant complication to our analysis due to the noise in the autocorrelation function as it approaches zero. The simulation results may serve as an evidence for the step function predicted by Hess; however, unavoidable noise in the tail of the autocorrelation function prohibits a stronger statement. In fact, the small negative numbers of autocorrelation functions cannot be even presented in the log scale.

C. Diffusion in Bidisperse Mixtures. Although the classic tube dilation theory is not applicable to our simulation, the concept of tube dilation should still be effective as long as the tube exists for the marginally entangled species. A tube constraint has been clearly demonstrated from the diffusion of middle beads in our previous work.[4] Diluting this marginally entangled PE chain (4.5K) should lead to the expansion of the tube, which is seen in Figure 8. The slowdown of middle bead diffusion for the pure 4.5K starts a little below 2 nm^2 in Figure 8, while the slowdown for the long-chain component in a

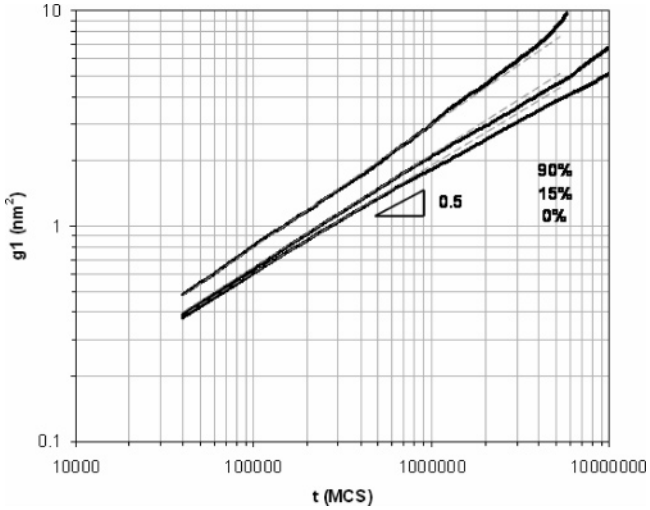

Figure 8. Example of middle bead diffusion of the long-chain components in mixtures with $c = 90\%$, 15%, and 0% from top to bottom, plotted against the time (dashed lines are illustrative straight lines).

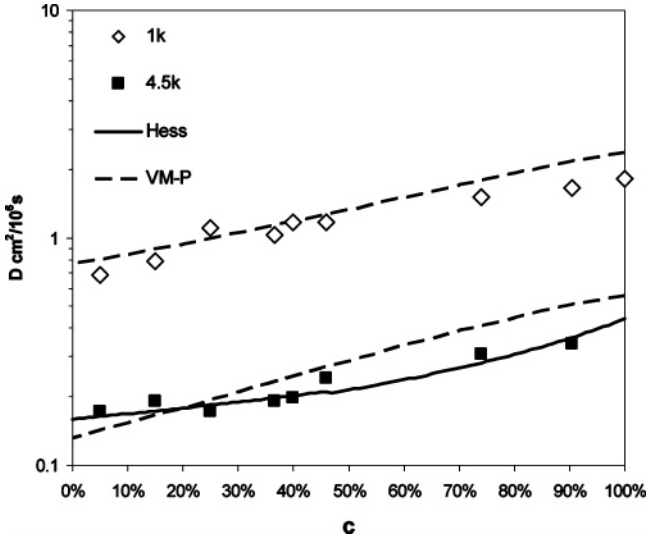

Figure 9. Diffusion coefficients of long-chain and short-chain components in the mixture plotted against the short-chain concentration, compared with the prediction of the Hess theory and the von Meerwall−Pearson model.

mixture with 15% short component starts at a larger time and distance scale. The long-chain component in a mixture with 90% short component does not show any intermediate slowdown at all as illustrated by dashed lines, which follow the initial slopes of each curve, and has a slope very close to 0.5. A more convincing determination of the tube diameter would require use of a significantly longer chain in the simulation.

Finally, we present the full range diffusion coefficients calculated from the trajectories of the center of mass of both short and long components. The results then have been fitted with both generalized Hess theory[26] shown in eq 7 and the von Meerwall/Pearson[25,27] model as shown in eqs 8, 9, and 13. Because M_c has been already decided as 1500 in our previous work,[4] there is only one fitting parameter in the generalized Hess theory. This parameter is the Rouse diffusion coefficient of the long-chain component D_t^R. In fact, according to the Hess theory, even D_t^R is not a fitting parameter because it can be obtained from the diffusion at the short time scale. Unfortunately, the Rouse diffusion of center of mass is largely inapplicable at very short time and distance scale. D_t^R cannot be faithfully exacted from the diffusion trajectory of the center of mass in the simulation because the center of mass diffusion does not follow the relationship msd $= 6D_t^R t^1$ at the short time scale as the theory expects. Of course, it is still possible to avoid using the fitting parameter here. As indicated in the literature,[30] if all diffusion coefficients obtained in the simulation are normalized by D_{pure} in monodisperse melts ($\Phi = 100\%$), D_t^R will disappear. However, for retaining the possibility of the direct comparison with future experimental data, the absolute diffusion coefficients are preferred so that D_t^R is still taken as a fitting parameter, which equals to 1.2 $cm^2/10^6$ s for the curve in Figure 9. In either way, we found the fitting agrees with our data very well using $N_c \sim 110$ ($M_c = 1500$). Note in the literature[26] a different N_c (~140) was adopted; however, the fitting did not completely agree with the experimental data. We found that the selection of N_c greatly affects the trend of the fitting curve. Hence, we believe that the inadequate description of experimental data of Hess theory shown in the literature is probably related to the choice of N_c instead of inadequacy of the Hess theory itself.

Our data have also been used in comparison with another theory by Pearson and von Meerwall[25,27] (von Meerwall/Pearson theory). This model is capable of describing not only the diffusion of long-chain molecules but also the diffusion of short-chain molecules. In addition to the parameters already determined[27] in conjunction with eqs 9 and 10, we have also used the fitting parameters $M_c = 1500$ and $R = 500$. In Figure 9, the von Meerwall/Pearson model fits the data very well when the long-chain molecule is the dominant component in the mixture. However, this theory somewhat overestimates the diffusion coefficients of short-chain molecules in pure melts, which leads to the small overestimation in the high content region of short molecules.

V. Summary

A recently developed dynamic Monte Carlo algorithm based on random two-bead moves has been used in simulating bimodal mixtures of PE with one marginally entangled component (~$3M_c$) and one unentangled component. The static and dynamic properties have been studied. As expected, there is no systematic change of mean-square radius of gyration as the concentration varies in the mixture. Thus, the mixture can be regarded as the Θ solution of the marginally entangled species.

At the initial stage for higher modes, the stretching parameter β in the KWW equation for different concentrations and different chain lengths falls onto a master curve against N/p. This behavior has been attributed to a local constrained dynamics due to intrachain interactions. For mixtures, β of long-chain component varies with the concentration. Below 25% of short-chain components, a plateau of β against N/p was found. Above 40%, no plateau can be clearly identified. The underlying physics between this plateau and the entanglement phenomena is still not clear. The effective relaxation times in KWW equation have been obtained as well. The local constrained dynamics results in an anomalous scaling for higher modes. This anomaly disappears after the Rouse or intermediate entangled dynamics sets in, depending on the chain length and concentration of the mixture. The mode analysis has been also used to check the Hess theory. The two-step relaxation of normal modes predicted by Hess theory can be vaguely identified but cannot be faithfully designated due to the data fluctuation in the decisive range of the autocorrelation function. The diffusion coefficients of both components in the mixture have been calculated and calibrated into the real time units over the full concentration range. The

diffusion coefficients increase with increasing short-chain concentration. The results have been tested against both the Hess theory and von Meerwall/Pearson model. Reasonable agreements have been reached.

Acknowledgment. This research was supported in part by the National Science Foundation under Grant DMR 04-55117.

References and Notes

(1) Padding, J. T.; Briels, W. J. *J. Chem. Phys.* **2002**, *117*, 925.
(2) Harmandaris, V. A.; Mavrantzas, V. G.; Theodorou, D. N.; Kroger, M.; Ramirez, J.; Öttinger, H. C.; Vlassopoulos, D. *Macromolecules* **2003**, *36*, 1376.
(3) Kremer, K. *Computational Soft Matter: From Synthetic Polymers to Proteins, Lecture Notes;* Attig, N., Binder, K., Grubmüller, H., Kremer, K., Eds.; John von Neumann Institute for Computing, Jülich, NIC Ser. *23*, 141−168, 2004.
(4) Lin, H.; Mattice, W. L.; von Meerwall, E. D. *J. Polym. Sci., Part B: Polym. Phys.* **2006**, *44*, 2556.
(5) Harnau, L.; Winkler, R. G.; Reineker, P. *J. Chem. Phys.* **1996**, *104*, 6355.
(6) Paul, W.; Smith, G. D.; Yoon, D. Y. *Macromolecules* **1997**, *30*, 7772.
(7) Baschnagel, J.; Binder, K.; Doruker, P.; Gusev, A. A.; Hahn, O.; Kremer, K.; Mattice, W. L.; Müller-Plathe, F.; Murat, M.; Paul, W.; Santos, S.; Suter, U. W.; Tries, V. *Adv. Polym. Sci.* **2000**, *152*, 41.
(8) Mavrantzas, V. G.; Theodorou, D. N. *Phys. Rev. Lett.* **2002**, *88*, 105503-1.
(9) Tsolo, G.; Mavrantzas, V. G.; Theodorou, D. N. *Macromolecules* **2005**, *38*, 1478.
(10) Watanabe, H.; Kotaka, T. *Macromolecules* **1984**, *17*, 2316.
(11) Struglinksi, M. J.; Graessley, W. W. *Macromolecules* **1985**, *18*, 2630.
(12) Green, P. F.; Kramer, E. J. *Macromolecules* **1986**, *19*, 1108.
(13) Doi, M.; Graessley, W. W.; Helfand, E.; Pearson, D. S. *Macromolecules* **1987**, *20*, 1900.
(14) Viovy, J. L.; Rubinstein, M.; Colby, R. H. *Macromolecules* **1991**, *24*, 3587.
(15) Wang, S. F.; von Meerwall, E. D.; Wang, S. Q.; Halasa, A.; Hsu, W. L.; Zhou, J. P.; Quirk, R. P. *Macromolecules* **2004**, *37*, 1641.
(16) Freed, D. E.; Burcaw, L.; Song, Y. Q. *Phys. Rev. Lett.* **2005**, *94*, 067602.
(17) Ferry, J. D. *Viscoelastic Properties of Polymers*; J. Wiley & Sons: New York, 1980.
(18) Doi, M.; Edwards, S. F. *The Theory of Polymer Dynamics;* Clarendon: Oxford, 1986.
(19) Kremer, K.; Grest, G. S.; Carmesin, I. *Phys. Rev. Lett.* **1988**, *61*, 566.
(20) Rouse, P. E. *J. Chem. Phys.* **1953**, *21*, 1272.
(21) Milner, S. T.; McLeish, T. C. B. *Phys. Rev. Lett.* **1998**, *81*, 725.
(22) Hess, W. *Macromolecules* **1987**, *19*, 1395.
(23) Hess, W. *Macromolecules* **1987**, *20*, 2587.
(24) Hess, W. *Macromolecules* **1988**, *21*, 2620.
(25) Pearson, D. S.; Fetters, L. J.; Graessley, W. W.; Ver Strate, G.; von Meerwall, E. *Macromolecules* **1994**, *27*, 711.
(26) Rathgeber, S.; Willner, L.; Richter, D.; Brulet, A.; Farago, B.; Appel, M.; Fleischer, G. *J. Chem. Phys.* **1999**, *110*, 10171.
(27) von Meerwall, E.; Feick, E. J.; Ozisik, R.; Mattice, W. L. *J. Chem. Phys.* **1999**, *111*, 750.
(28) Park, S. J.; Larson, R. G. *Macromolecules* **2004**, *37*, 597.
(29) Baschnagel, J.; Paul, W.; Tries, V.; Binder, K. *Macromolecules* **1998**, *31*, 3856.
(30) Harmandaris, V. A.; Mavrantzas, V. G.; Theodorou, D. N. *Macromolecules* **1998**, *31*, 7934.
(31) Barsky, S. *J. Chem. Phys.* **2000**, *112*, 3450.
(32) Rapold, R. F.; Mattice, W. L. *J. Chem. Soc., Faraday Trans.* **1995**, *91*, 2435.
(33) Doruker, P.; Mattice, W. L. *Macromolecules* **1998**, *31*, 1418.
(34) Mattice, W. L.; Suter, U. W. *Conformational Theory of Large Molecules: The Rotational Isomeric State Model in Macromolecular Systems*; Wiley: New York, 1994.
(35) Cho, J.; Mattice, W. L. *Macromolecules* **1997**, *30*, 637.
(36) von Meerwall, E.; Beckman, S.; Jang, J.; Mattice, W. L. *J. Chem. Phys.* **1998**, *108*, 4299.
(37) Shaffer, J. S. *J. Chem. Phys.* **1995**, *103*, 761.
(38) de Gennes, P. G. *Macromolecules* **2002**, *35*, 3785.

MA062088S